FACULTY OF HYSICS
BABES-BOLYAI UNIVERSITY
CLUJ-NAPOCA

Doctoral Thesis Summary

Contributions to application of the photodynamic therapy (PDT) in oncology

by

Andreea Dimofte

Scientific Advisor
Prof. Dr. Onuc Cozar

CLUJ-NAPOCA
2011

Contents

Keywords:optical properties of tissues, photodynamic therapy, cancer therapy

Chapter I Introduction

Traditional cancer treatments include radiation, surgery and/or chemotherapy all of which have deleterious side effects. As an alternative to these treatments the photodynamic therapy (PDT) offers a more targeted and less invasive treatment.

The main objectives of this thesis were to investigate and to improve the methods of quick and accurate determination of the optical properties of tissues in order to use the photodynamic therapy for various cancer treatments.

In Chapter II, Modern techniques in radiation therapy, some of the specialized techniques used in radiation therapy of the cancer are described.

Chapter III, Principles of the photodynamic therapy, displays the main physical processes and parameters of the PDT in order to characterize and use this method in the therapy of the cancer. The diffusion theory and the calibration of isotropic light dosimetry probes are examined.

Chapter IV *The photodynamic therapy (PDT): Determination of the optical properties of the tissue* describes the methods and the approximations used in this thesis in order to determine the optical properties of the tissues. The detector calibration factor, β, for interstitial *in-vivo* light dosimetry is determined using isotropic detectors with scattering tip. Quick and accurate determination of the absorption and scattering properties interstitially in turbid media and then the determination of optical properties in a heterogeneous turbid media using a cylindrical diffusing fiber (CDF) are discussed. In the last paragraph the determination of the detector calibration factor and the light dosimetry at tissue surfaces for small circular fields were presented.

The chapter *V. The photodynamic therapy: application to the various cancer treatments,* describes the PDT treatment of the prostate, of the malignant pleural effusion (lung cancer) and head and neck cancer. In the last part of this thesis the conclusions and the references are presented.

.

Chapter II Some modern techniques in radiation therapy of cancer

This chapter describes some of the specialized techniques used in radiation therapy of the cancer. These techniques deal with specific problems that require either equipment modification, quality assurance or require special clinical support. We can distinguish two categories of specialized techniques: special dose delivery techniques or special

target localization techniques. There are several techniques and among those the following methods are described:

II.1.Stereotactic irradiation. This term is used to describe focal irradiation techniques that use multiple non-coplanar photon radiation beams and deliver a prescribed dose of ionizing radiation to preselected and stereotactically localized lesions, primarily in the brain.

II.2. Conformal radiotherapy and intensity modulated radiotherapy. In comparison with standard dose delivery techniques, conformal radiotherapy improves the tumor control by using special techniques that allow the delivery of a higher tumor dose while sparing the normal tissue.

II.3. Image guided radiotherapy (IGRT). The ideal image guided system will allow the acquisition of soft tissue images at the time of each fraction of radiotherapy. The system must be fast and simple so as not to affect appreciably the patient throughput on the treatment machine.

II.4. Respiratory gated radiotherapy (RGR). To account for organ motion during treatment, 4-D imaging technology is required, which allows viewing of volumetric CT images changing over the fourth dimension, time.

II.5. Positron emission tomography/computed tomography (PET/CT) scanners and positron emission tomography/computed tomography image fusion. PET provides information on the metabolic function of organs or tissues by detecting how cells process certain compounds such as glucose. The CT scanner is based on acquisition of a large number of cone beam projections around a patient by a detector array and representation of transmission measurements of X rays through a patient. The measured transmission data are reconstructed to produce a tomographic image, most commonly through the filtered backprojection method. PET/CT machines combining the strengths of two well established imaging modalities represent the most exciting innovation in cancer diagnosis and therapy.

II.6. Photodynamic therapy (PDT). Photodynamic therapy is a light-activated chemotherapy in which light is used to activate a photosensitive drug that has accumulated within cells such that it causes oxidative injury to the cells. Unlike traditional chemotherapy, which has a systemic effect, PDT achieves a localized effect. In this sense, PDT is more like a surgical or radiation therapy technique than a chemotherapeutic treatment.

Chapter III. Principles of photodynamic therapy (PDT)

III.1. Introduction

Photodynamic therapy (PDT) is a light-activated chemotherapy in which light is used to activate a photosensitive drug that has accumulated within cells such that it causes oxidative injury to the cells. The basic ingredients for a successful PDT treatment are: (1) drug, (2) light, and (3) oxygen. A photon is absorbed by a photosensitive drug that moves the drug into an excited state. The excited drug can then pass its energy to oxygen to create a chemical radical called "singlet oxygen". Singlet oxygen attacks cellular structures by oxidation. Such oxidative damage might be oxidation of cell membranes or proteins. When the accumulation of oxidative damage exceeds a threshold level, the cell begins to die.

Photodynamic therapy depends on the amount of light delivered (L), the amount of photosensitizing drug (D) in the tissue, and the amount of oxygen (O_2) in the tissue.

Photodynamic therapy involves optical irradiation of photosensitized biological tissues [*van Hillegersberg et al* 1994]. The activation of a photosensitizer is determined by the product of the absorption coefficient of the photosensitizer in the tissue and the light energy fluence. The latter is a measure of the amount of optical energy that is available for absorption by the photosensitizer. In most tissues and at most wavelengths of interest for PDT the optical scattering coefficient is large relative to the absorption coefficient. Due to scattering, within the tissue the light is moving in all directions. Summing the radiance over all directions in space yields the energy fluence rate Ψ (called the fluence rate). To measure Ψ requires a detector that accepts light isotropically, that is the response is identical for light incident on the probe from all directions. Such an *isotropic light detector* (also referred as an isotropic light dosimetry probe, an isotropic probe etc) may consist of a light scattering bulb about 1 mm or less in diameter connected to a fiber with appropriate read-out electronics.

III.2. Diffusion theory used for non-invasive determination of tissue optical properties

The diffusion model for determination of the optical properties of tissues developed by Farrell, Patterson and Wilson [*Farrell 1992*] is described. The goal of their work was to develop a non-invasive technique to determine the optical properties of tissue using diffuse reflectance. The optical properties of tissue are used then to calculate the fluence distribution of light during therapeutic procedures such as

photodynamic therapy [*Wilson 1986*] or laser therapy [*Jaques 1987*]. The concentration of PDT photosensitizing agents in tissue can be determined from the absorption coefficient [*Patterson 1987*], while metabolic processes can be monitored by measuring changes in the tissue optical properties due to changes in hemoglobin oxygenation [*Cope 1988*]. The dependence of the diffuse reflectance *R(r)* on the radial distance from the light source is determined using different physical models. If this dependence is established, the absorption coefficient μ_a and the transport scattering coefficient $\mu_s' = (1\text{-}g)\,\mu_s$ can be determined. The transport scattering coefficient μ_s' is introduced in order to reduce the determination of photon transport due to anisotropic scattering to that of isotropic scattering; μ_s is the anisotropic scattering coefficient and *g* is an anisotropy parameter equal to the average scattering cosine. Some authors [*Groenhuis 1983a,b, Steinke 1986, Patterson 1989a, Schmitt 1990*] developed various models to determine the optical properties of tissues.

Farrel et al. [*Farrel 1992*] proposed a technique which depends only upon the shape of the radial reflectance curve, i.e., a relative reflectance measurement, in order to determine the optical properties of the tissue. Two different scatter source geometries were studied: one is a single isotropic scattering site and the other is an exponentially weighted line source of isotropic scattering sites. The dipole source model was modified to account for the correct boundary conditions.

As a *summary*, a non-invasive technique to determine the optical properties of tissue using diffuse reflectance was described. The phantom data, as the Monte Carlo data, indicate that the single scatter source model described by:

$$R_d(z_0) = \frac{a'}{2}\left(1 + e^{-(4/3)A\sqrt{3(1-a')}}\right)e^{-\sqrt{3(1-a')}} \qquad \text{(III.2.1)}$$

is adequate to describe the reflectance. This expression includes only three independent parameters: μ_t^r, μ_{eff} and A. $\mu_{eff} = [3\,\mu_a(\mu_a + \mu_s')]^{1/2}$ *is* the *effective attenuation coefficient*, $A = (1 + r_d)/(1 - r_d)$ is related to the internal reflection, r_d is a parameter that depends on the relative refractive index of the tissue-air interface [*Groenhuis1983a, b*]. The *transport albedo* is $a' = \dfrac{\mu_s'}{\mu_a + \mu_s'}$. The value of A is determined by the relative refractive indices of the tissue and the probe and can be considered to be constant for a

given probe, since the refractive index of tissue is constant to within a few percent in the visible wavelength range. This suggests that the absorption and transport scattering coefficients can be determined by fitting the reflectance data to eq. (III.2.1) to yield μ_t^r and μ_{eff} *directly* and, thereby, μ_s^r and μ_a.

III.3. Calibration of the isotropic light dosimetry probes

To measure the fluence rate (Ψ) requires a detector that accepts light isotropically, that is the response is identical for light incident on the probe from all directions. An isotropic light detector consists of a light scattering bulb about 1 mm or less in diameter connected to a fiber with appropriate read-out electronics.

The isotropic probe based on a scattering bulb is usually calibrated in a collimated light beam *in air* and depends on the refractive index (n_m) of the medium relative to that of the probe bulb material (n_b). Experimentally, a calibration curve can be determined to correct the probe reading for measurements in *clear* media with different refractive indices. Measurements with the probe in a *turbid* (scattering) medium with refractive index, absorption coefficient and scattering coefficient different from those of the probe bulb may require additional corrections [*Marijnissen 1993*]. The principle of calibration in a collimated beam and in completely diffuse light in air using an integrating sphere are described. It was concluded that the probe response is the same for collimated and diffuse light within the bounds of experimental error.

III.4. Light Distributions from Point, Line and Plane Sources for Photochemical Reactions and Fluorescence in Turbid Biological Tissues

In order to interpret the photochemical reactions the light distribution in the reaction medium has to be known. The light source can be: an isotropic point source with spherically symmetric light fields, a line source with cylindrically symmetric light fields, and a plane source with one-dimensional variation in light fields. Jacques [*Jacques 1998*] developed simple expressions for steady-state light transport due to point, line and plane sources and illustrated how they pertain to fluorescence measurements and PDT. The diffusion theory expressions were compared with Monte Carlo simulations. A major conclusion of this study is that the shape of the fluence rate distributions due to point, line, and plane sources are accurately described by the diffusion theory equations, however the absolute values of the fluence rates are poorly predicted.

Chapter IV The photodynamic therapy (PDT) - determination of the optical properties of the tissues

IV.1. Introduction

Determination of tissue optical properties is a critical factor in planning interstitial light source placement. In order to evaluate the PDT efficacy the drug concentration has to be known. The scattering and absorption properties of the tissue are characterized by the transport scattering (μ_s') and absorption (μ_a) coefficients.

The light fluence rate Φ at a distance r from a point source of source strength, S, can be expressed as [*Jacques 1998*]:

$$\Phi(r) = \frac{S.\mu_{eff}^2}{4\pi r \mu_a} e^{-\mu_{eff} r} \quad \text{or} \quad \Phi(r) = \frac{3S\,\mu_s'}{4\pi r} e^{-\mu_{eff} r} \qquad \text{(IV.1.1)}$$

where: S is the strength of the point source, $\Phi(r)$ is the fluence rate at position r, $\mu_{eff} = \sqrt{3\mu_a \mu_s'}$ is the effective attenuation coefficient in tissues.

The scheme of the measurement geometry, illustrating the setup for measurement of distribution of light fluence rate, optical properties and diffuse absorption spectra is described [*Zhu 2005c*]. The distribution of light fluence rate was determined by moving the detector in a catheter along the light source. The magnitude of the fluence rate near the light source is determined by μ_s' only and the slope of the spatial decay of the light fluence rate is determined by μ_{eff} only. These investigations [*Zhu 2005c*] demonstrated the inter- and intra-prostate variation of optical properties and MLu tissue concentration. The variation of the optical properties can be used to explain the observed variation of light fluence rate in the studied tissue. Given this heterogeneity, a real-time dosimetry measurement and feedback system for monitoring light fluences during treatment should be considered for interstitial prostate PDT studies.

The main objective of the studies described in the following paragraphs is to demonstrate the feasibility of measuring the distribution of dosimetric parameters for PDT *in vivo*, namely the tissue optical properties, tissue concentration of drug, and tissue oxygenation. Measurements were made before, during and after PDT. Differences within and between patients were also evaluated. These parts represent the contribution of the author of this thesis to the improvement and application of the PDT for various cancer treatments.

IV.2. Determination of the optical properties of various media.

Isotropic detectors are used in clinical PDT as interstitial *in-vivo* dosimeters. The response of an isotropic detector is, however, a function of the indices of refraction of the surrounding medium and the scattering bulb because the signal detected by the isotropic detector depends on the amount of light transmitted into the scattering bulb from the surrounding medium. It is important to know how the detector calibration factor depends on the properties of the surrounding medium.

IV.2.1. Detector calibration factor for interstitial in-vivo light dosimetry using isotropic detectors with scattering tip[Zhu& Dimofte et al 2005b]

The detector calibration factor, β, for a detector merged in a medium at depth *d* is determined by measurements at four points:

$$\beta = \frac{\Phi_{air}(d_{ref})}{\Phi_{wat}(d)} \frac{\Phi_0(d)}{\Phi_0(d_{ref})} \qquad \text{(IV.2.1.1)}$$

where

- $\Phi_{wat}(d)$ and $\Phi_{air}(d_{ref})$ are the light fluence rates measured in water and in air, respectively, at depth d and d_{ref}.
- $\Phi_0(d)$ and $\Phi_0(d_{ref})$ are the light fluence rates measured in air at the same locations.

The experimental setup to determine the detector calibration factor, β, is shown in Fig. IV.2.1.1.

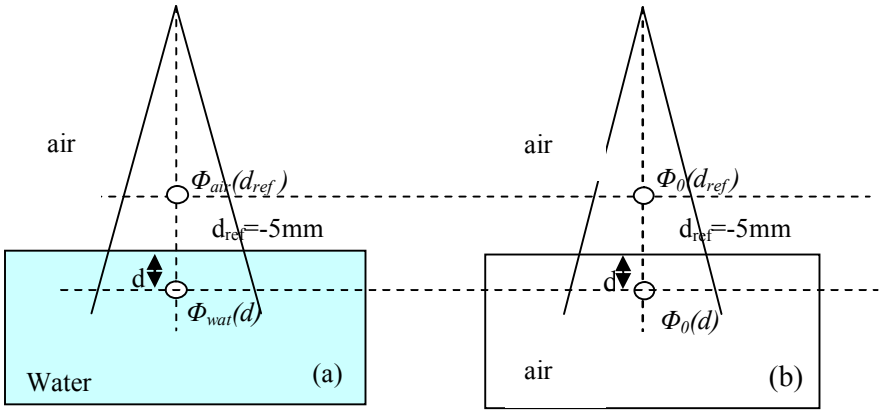

Figure IV.2.1.1. *The experimental setup used to determine the detector calibration factor [Zhu& Dimofte et al 2005b]*

To determine the influence of the catheter on the detector calibration factors, β is measured for three different geometries: (a) detector in water-filled catheter in water; (b) detector in air-filled catheter in water; (c) detector in water-filled catheter in air.

The obtained results are compared to β measured for the bare isotropic detector without a catheter. These experiments are designed to test whether the detector calibration factor is determined by the immediate surrounding medium of the detector or by the outmost medium. Additional experiments are performed to determine the variation of β when the detector position is varied from touching the catheter wall closest to the light source, to not touching, to touching the catheter wall farthest from the light source.

In order to find a formula for the correction factor which can be used for experimental determination the diffusion theory described in chapter III was used. A model for two and three layered medium are developed *[Zhu& Dimofte et al 2005b]*. Using the experimental method described at the beginning of the paragraph, the detector calibration factor was determined for three different types of isotropic detectors (without catheter). The correction factor β was then determined for air-water interface and in uniform medium of water. The experimental values are shown in figure IV.2.1.2. As expected, the correction factor is reduced at the air–water interface. The measured value is 13-14% lower than the average of β in water and in air for all detector types.

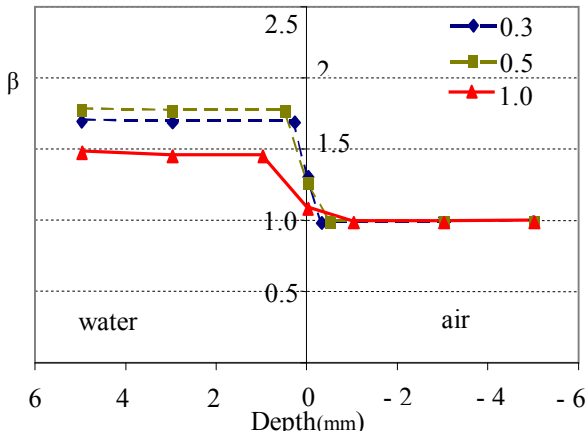

Figure IV.2.1.2*. Detector calibration factor, β, measured at different depths from an air-water interface for three isotropic detectors with different radius.[Zhu & Dimofte et al 2005b]*

When isotropic detectors are used inside a catheter, the value of the detector calibration factor β is determined by the outmost medium rather than the immediate surrounding medium of the isotropic detector.

The theory predicted that the index of refraction (n_c) for the intermediate medium surrounding the isotropic detector has no impact on the detector calibration factors and is independent of the ratio of the radius (r_c / r_2). The influence of the effect of the detector touching the catheter wall was also examined.

From this study results that the detector calibration factor is determined by the index of refraction of the outmost medium surrounding the isotropic detector, rather

than the immediate medium surrounding the detector. Theoretical analysis demonstrated that the effect of intermediate medium is negligible.

IV.2.2. Interstitial determination of absorption and scattering coefficients

The goal of bellow presented study [*Dimofte 2005*] is to develop an interstitial method that can be used *in vivo* to quickly determine both the absorption and the reduced scattering coefficients of tissue using a spatial CW method. For this, a device to quickly determine tissue optical properties by measuring the ratio of light fluence rate to the source power along a linear channel at a fixed distance (5 mm) from an isotropic point source was developed. Diffuse light is collected by an isotropic detector whose position is determined by a computer-controlled step motor, with a positioning accuracy of better than 0.1 mm. The result is fitted with a diffusion equation, using a nonlinear optimization algorithm, to determine μ_a and μ_s'. This method has been applied to *in vivo* optical property measurements in human prostate.

A. Experimental set-up for broad beam measurements

The measurement set-up is shown in figure IV.2.2.1. The measurements were made under five different conditions: one for Liposyn solution, three for Liposyn solution plus three ink concentrations with known optical properties, and one for pure water. The values of μ_a determined by this method and those expected based on the known ink concentrations agreed to within 8%.

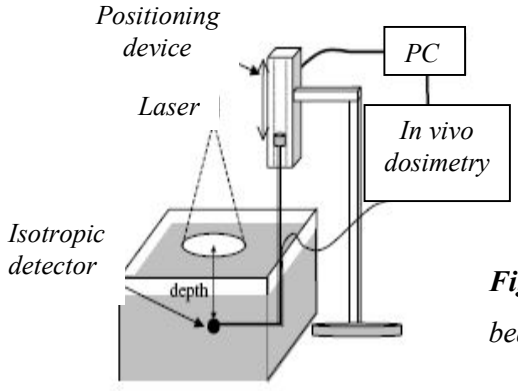

***Figure IV.2.2.1**. Experimental set-up for broad beam measurements. [Dimofte et al. 2005]*

The tissue simulating phantoms are made of separate scattering and absorbing components. Using the broad beam method, nine tissue simulating phantoms with Liposyn concentrations of: (A) 0.23%, (B) 0.53% and (C) 1.14% and ink concentrations of: 0.002%, 0.012% and 0.023% were investigated. Figure IV.2.2.2 shows the results for one phantom (A). The best fit scattering coefficients were: 1.73 cm^{-1} (with absorption coefficients of 0.10, 0.48 and 1.00 cm^{-1}).

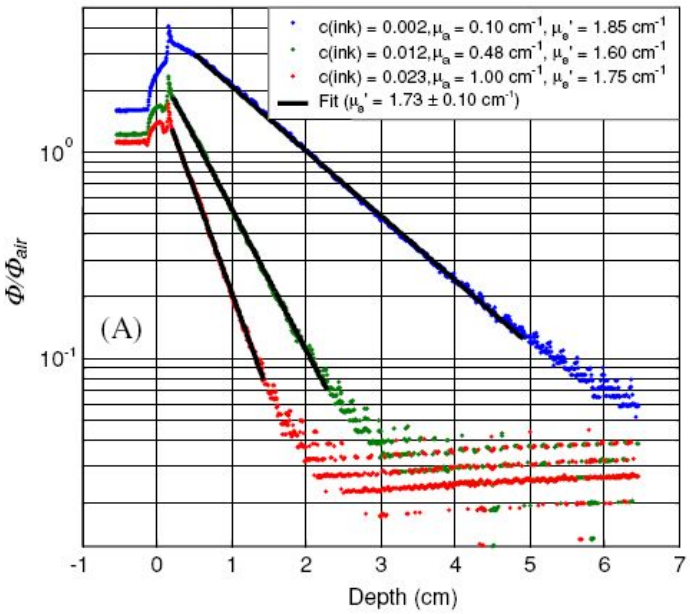

Figure IV.2.2.2. *Optical properties characterization using broad beam method. Symbols represent measurements with an isotropic detector. Solid lines are the best fit.*

B. Interstitial measurements

Description of the interstitial set-up for phantom measurement

The experimental set-up for the parallel-catheter measurement system is shown in figure IV.2.2.3. Table IV.2.2.1 summarizes the optical properties (μ_a, μ_s', h) obtained using the parallel catheter measurements and those obtained from broad-beam measurements in the same phantoms (A).

Table IV.2.2.1. *A comparison between optical properties (μ_a, μ_s', μ_{eff}) determined by broad-beam and parallel-catheter methods for one optical phantom with Liposyn concentrations: (A) 0.23%, and ink concentrations (0.002%, 0.012% and 0.023%) for three different separations (h) between the catheters.*

Separation	Parallel catheters				Broad beam			Difference (%)		
	h	μ_a	μ_s'	μ_{eff}	μ_a	μ_s'	μ_{eff}	μ_a	μ_s'	μ_{eff}
A h=3mm	2.5	0.10	2.04	0.77	0.10	1.73	0.72	2.0	14.0	6.9
		0.47	2.11	1.72	0.48	1.73	1.58	5.1	17.9	7.5
		0.93	2.49	2.64	1.00	1.73	2.28	8.6	39.1	15.8
h=5mm	4.5	0.11	2.04	0.82	0.10	1.73	0.72	8.0	17.9	13.9
		0.53	2.21	1.87	0.48	1.73	1.58	9.4	27.7	18.4
		1.10	2.19	2.75	1.00	1.73	2.28	9.9	32.4	20.6
h=7mm	6	0.11	1.93	0.79	0.10	1.73	0.72	9.0	7.8	9.7
		0.55	1.91	1.78	0.48	1.73	1.58	12.7	6.7	11.3
		1.18	1.49	2.29	1.00	1.73	2.28	15.2	16.8	0.4

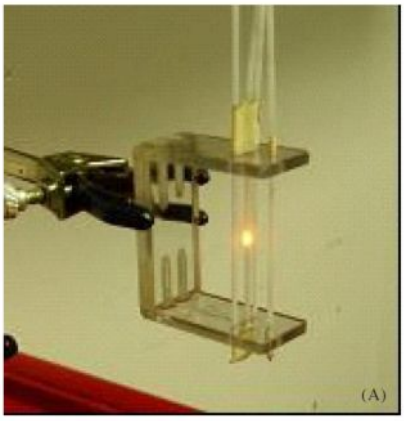

(A) Picture of the optical property device consisting of 4 parallel catheters positioned at 3 different distances (3, 5 and 7 mm) from the central catheter. The light source is placed in the centre catheter, while the detector is moved along each catheter, positioned at different distances from the light source.

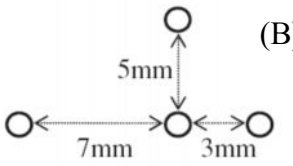

(B) Top view of the optical property device pictured in (A).

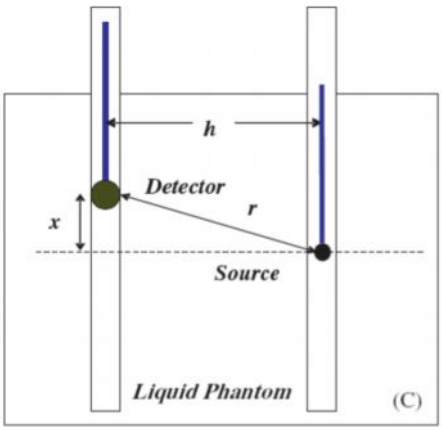

(C) Schematics of the light source and detector placement. The distance between the light source and the detector is h.

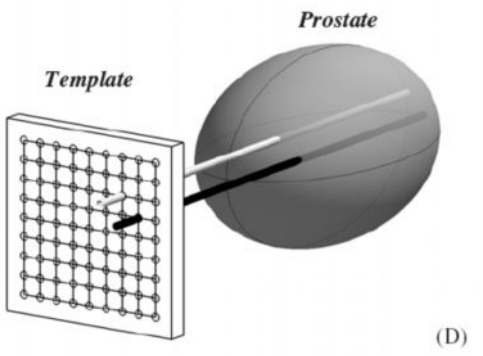

(D) Diagram of catheter positioning during prostate PDT.

***Figure IV.2.2.3**. Experimental set-up for the parallel-catheter measurement system*

Optical properties of the prostate tissue, namely μ_a, μ_s' and $\delta = 1/\mu_{eff}$ were also measured in 11 patients with locally recurrent prostate carcinoma using the interstitial set-up. Table IV.2.2.2 summarizes the measured optical properties in human prostate for 11 patients [*Zhu &Dimofte 2005a*].

Table IV.2.2.2. *Summary of optical properties measured in human prostate. The values in parentheses are the standard deviation of the mean values measured from different locations in the same prostate. No standard deviation is listed if only one data point is available. (∗ represents the measurements done with the motorized probe.)*

Patient number	μ_a (cm^{-1})	μ_s' (cm^{-1})	δ (cm)
1	0.09	29.8	0.34
2	0.15	22.0	0.31
3	0.43(0.28)	7.69 (4.76)	0.41
4	0.21	11.8	0.37
5	0.27 (0.27)	10.5 (11.2)	0.50 (0.05)
6*	0.53 (0.36)	6.61 (4.51)	0.41 (0.09)
7*	0.63 (0.32)	4.62 (2.870	0.42 (0.10)
8*	0.67 (0.17)	6.39 (3.18)	0.32 (0.10)
9*	0.71 (0.43)	8.99 (6.51)	0.32 (0.12)
10*	0.27 (0.14)	18.5 (11.6)	0.30 (0.07)
11*	0.72 (0.11)	3.37 (1.37)	0.39 (0.11)

The main objective of this study was to create a device that can assess the optical properties (scattering and absorption coefficients) *in vivo* by interstitial measurements. This device was tested in tissue-simulating phantoms with different optical properties. During *in vivo* measurement, the scanning distance is typically 5 cm, so each measurement of optical properties takes 4 s. This is the time required to obtain a useful data set. Extensive commissioning of the device has been performed to ensure the accuracy of the measurement at this speed. The results of these measurements were compared with optical properties determined by an *ex vivo* method.

IV.2.3. Determination of optical properties in a heterogeneous turbid media using a cylindrical diffusing fiber

The objective of this study *[Dimofte et al 2008]* was to examine the feasibility and accuracy of using the CDF to characterize the absorption (μ_a) and reduced scattering (μ_s') coefficients of heterogeneous turbid media. Measurements were performed in homogeneous and inhomogeneous prostate simulating phantoms. Linear sources of various lengths (1 to 5cm long) were placed in the phantom, through transparent catheters.

Description of the interstitial set-up for phantom measurement

Linear light sources of different lengths (1, 2, 3, 4 and 5cm) were placed inside the phantom through a catheter (figure IV.2.3.1). Optical fiber-based isotropic detectors are used.

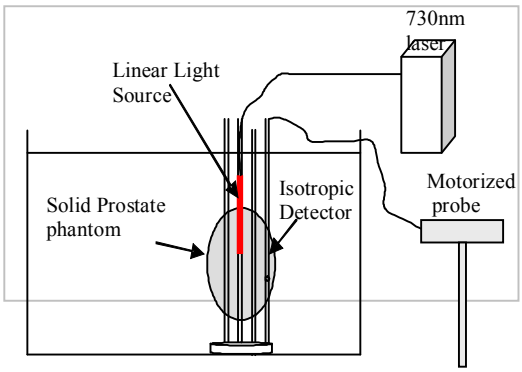

Figure IV.2.3.1. *Experimental setup using homogeneous phantoms*

Measurements were also taken in a prostate phantom (figure IV.2.3.2a). Placement of the light sources and detectors throughout the prostate is shown in figure. During the treatment we divided the prostate into zones A and B and then into 9 zones (don't show in figure). Cylindrical diffusing fibers varying in length from 1cm to 5cm were used as light sources. The CDF were placed in the phantom through transparent catheters.

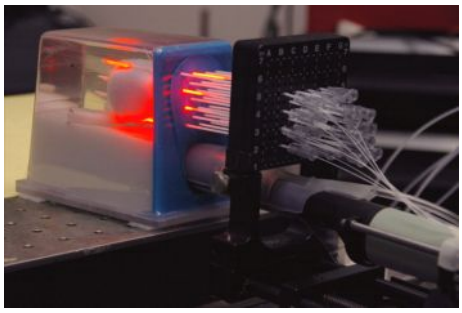

Figure IV.2.3.2. (a) Experimental setup for prostate measurement showing the placement of catheters inside the prostate.

(b) Diagram showing the needle positioning and inhomogeneity placement throughout the phantom.

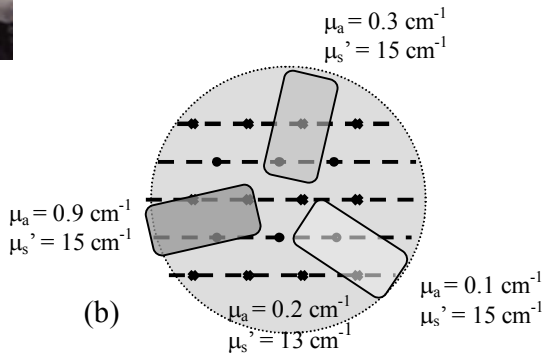

(b)

Figure IV.2.3.3 shows the light distribution in-air, measured using an isotropic detector along linear sources of different lengths (2, 3 and 4 cm). The distance between the source and detector was kept 7mm.

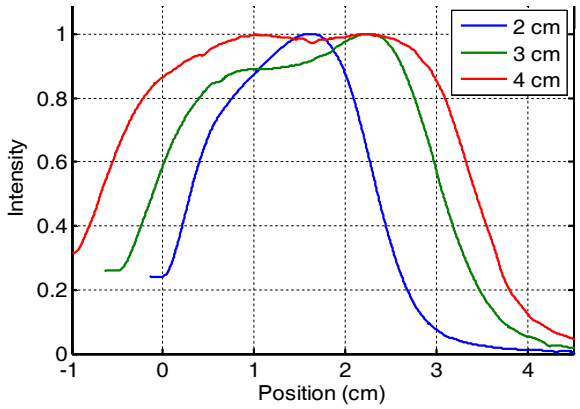

Figure IV.2.3.3. *Light distribution measured along a 2, 3 and 4cm long linear light source placed 7mm from the isotropic detector in air. The intensity was normalized to be 1 at the maximum value.*

In fig. IV.2.3.4a one can see the profile obtained from the detector placed in zone one from the linear light source 1. The dots represent the data, the red line is the fit and the dotted blue line shows the in air scan of that particular light source. Fig. IV.2.3.4b plots the absorption coefficient as determined along the linear light source (4 cm in length).

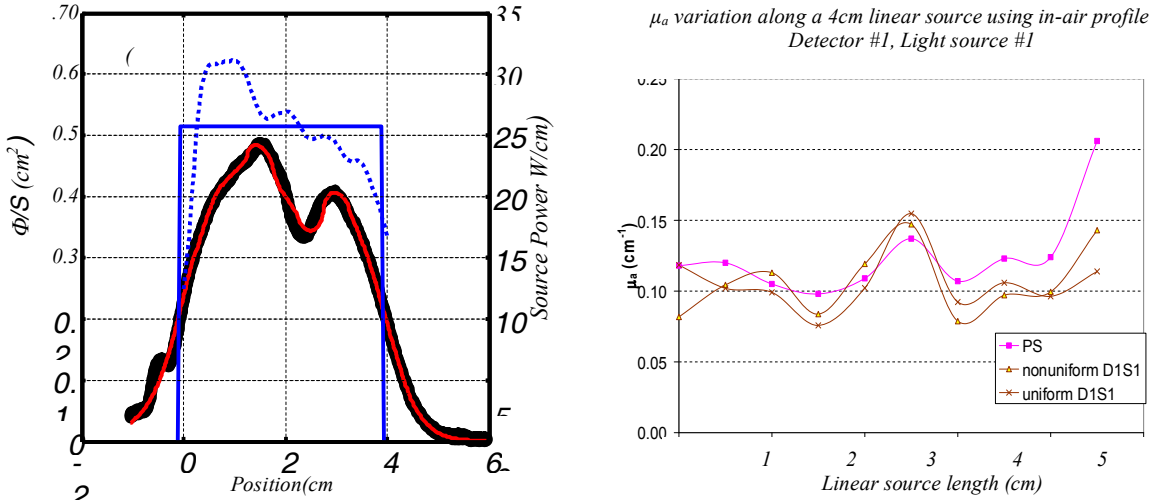

Fig.IV.2.3.4.(a) Fluence profile and (b)comparison between μ_a obtained using in-air profile and using uniform profile for source 1 and detector 1.

Taking into account the obtained results we can say that it is possible to determine the optical properties of inhomogeneous samples using the same linear sources used for interstitial PDT treatment. The sensitivity for determination of μ_s' is quite poor using linear sources, however heterogeneities in the absorption coefficient can be quantified. The effect of variations in the intensity profile of the linear light source on determination of the μ_a is relatively small, allowing the use of a generic light source profile for clinical measurements. The error decreases in very heterogeneous turbid media because of the presence of unique features.

IV.2.4. Light dosimetry in various media

IV.2.4.a. Determination of the blind spot correction factor, F_b

The objectives of this study *[Dimofte 2002]* are the following: (1) to estimate the effective attenuation coefficient (μ_{eff}) from the ratio of measured fluence rate to incident fluence rate in air, *Φ/Φair*. The value μ_{eff} can be used to determine the optical penetration depth (δ) inside the tissue; (2) to examine the spatial variation of measured light fluence rate on tissue surface during MLu-mediated PDT on chest wall; (3) to examine the time dependence of light fluence rate during chest wall PDT; (4) to estimate the optical properties of the tissues exposed to light *in vivo* during the chest wall PDT treatment and to estimate the effective depth of light penetration; (5) to study the variation of ratio *Φ/Φair* on the beam radius and depth, in order to use PDT to treat small lesion.

A practical isotropic detector does not respond to light isotropically. As a result, an isotropic detector may underestimate the ratio between total light fluence and incident light fluence [*Marijnissen 1996*]. The detector calibration factor, F_b, is defined as the ratio between the true ratio and measured ratio of the fluence: $F_b = \frac{(\Phi/\Phi_{air})_{meas}}{(\Phi/\Phi_{air})_{true}}$

To determine the detector calibration factor, F_b, the isotropic detector response for an ideal Lambertian surface with total diffuse reflectance (R_d) of 1 was measured.

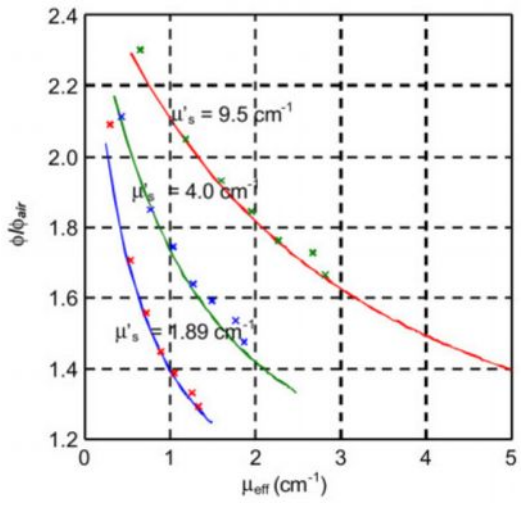

Figure IV.2.4.1*. The ratio of the measured fluence rate to incident fluence rate at the surface of the phantom as a function of μ_s' and μ_{eff}. Each "x" symbol represents a separate measurement. The theoretical curves have been corrected by the mean detector calibration factor β = 0.86 measured specifically for the 1-mm diameter isotropic detectors used in these studies. [Dimofte 2002]*

In order to estimate the effective attenuation coefficient (μ_{eff}) from the ratio of measured fluence rate to incident fluence rate in air, *Φ/Φair*, measurements were performed in liquid optical phantoms with the same treatment conditions as those used during in-vivo measurements. The ratios of the measured fluence rate to the incident

fluence rate at the surface of the phantom as a function of the reduced scattering (μ_s') and effective coefficients (μ_{eff}) are shown in figure IV.2.4.1. Three intralipid concentrations were used: 0.12%, 0.3%, and 0.6%. Seven ink concentrations were used: 0%, 0.007%, 0.014%, 0.0215%, 0.028%, 0.035%, and 0.042%.

Chest wall PDT and in vivo light fluence measurements

The objective of this study *[Dimofte 2002]* is to determine the spatial and time dependence of the measured light fluence rate *in situ* in patients enrolled in the ongoing Phase II trial of MLu mediated chest wall PDT for recurrent breast cancer. Five patients with recurrent cutaneous breast cancer were enrolled in a Phase II clinical trial of MLu mediated chest wall PDT treatment. All treatments were delivered with the same incident fluence rate of 75 mW/cm^2 determined by total light energy divided by the treatment area. The total treatment time was 2000 seconds, corresponding to a total incident light irradiance of 150 J/cm^2. 730 nm light was produced by a 15 W Diode Laser. Our data shows that there were considerable spatial variations of the fluence rate distribution within the treated sites, Figure IV.2.4.2. demonstrates this.

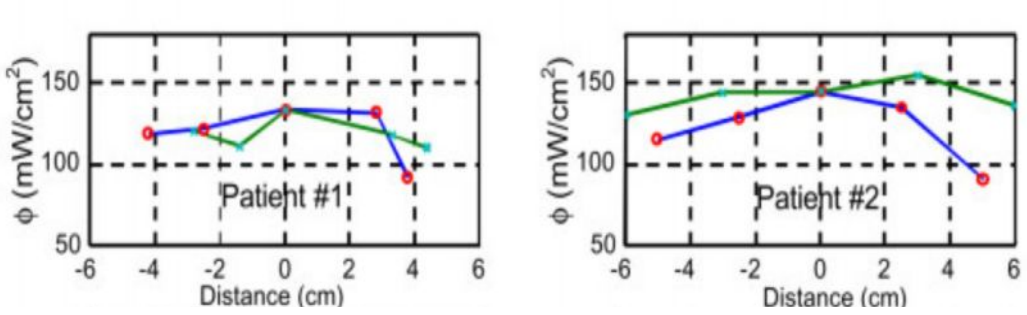

Figure IV.2.4.2. *Lateral light fluence rate (Φ) distribution on chest wall for two patients treated. x denotes the horizontal distribution along the patient's lateral direction, o denotes the vertical distribution along the patient's superior-inferior direction. The circular treatment diameters for the five patients were 9, 12, 11, 12 and 9 cm, respectively* [*Dimofte 2002]*

Very little time dependence of fluence rate was observed. The conversion factor to convert incident light fluence rate to light fluence rate on tissue surface, including tissue backscattering, was determined to be 1.6 ± 0.2 for five patients receiving MLu-mediated PDT. However, because of heterogeneity of optical properties, the actual fluence rate on patients varied by 73% (1.1–1.9). A spatial variation of Φ of a similar magnitude (70%) was observed. This is attributed mostly to variation of optical properties in patients. There are significant increases (up to 2 times) in measured light fluence rate versus

calculated incident fluence rate, and consequently all PDT chest wall treatment protocols incorporate careful *in-vivo* light dosimetry.

Treatment based on output of light alone seriously underestimates available light at tissue surface, which varies significantly depending on treatment patient optical properties and, to a lesser extent, patient contour, and may affect treatment outcome.

IV.2.4b. Light dosimetry at tissue surfaces for small circular fields [*Zhu &Dimofte et al 2003*]

When treating the surface lesions with PDT, it is often necessary to treat a lesion as small as 2-cm in diameter. For these small fields, the light fluence rate reduces significantly from that for an infinite large field because of the reduced photon scattering by tissue. The clinical questions to ask are: (1) how does the light fluence rate change with field size, given similar treatment conditions and (2) what lateral extent of the light field is sufficient to cover the tumor at depth in tissue?

The ratio between the light fluence rate and the incident irradiance Φ/Φ_{air} as a function of the tissue optical properties for a broad laser beam incident on the skin surface, both inside and outside tissue was determined by [*Dimofte 2002*]. Now we extend the relationship to a light field with a finite circular dimension.

The light fluence rate above the tissue surface is calculated using the diffuse reflectance R_d as was described in this paragraph and [*Simada 2001, Vulcan 2000*, *Dimofte 2002*, *Zhu &Dimofte et al 2003*] using the relations:

$\frac{\Phi}{\Phi_{air}} = 1 + R_d$, where R_d is the diffuse reflectance $R_d = \int_0^{90^0} r_d \, d\theta$ and θ is emitting angle. The phantom measurements (with known optical properties) were performed in a liquid phantom made of intralipid (0.25, 1, 1.5%) and ink to verify the Monte-Carlo results. Series of circular fields (radius R = 0.25, 0.35, 0.5, 0.75, 1, 1.5, 2, 3 cm), defined at the phantom surface, were produced by a circular block made of blackened paper. The comparison between measurements and Monte-Carlo simulations on a semi-infinite medium is shown in Figs. IV.2.4.3.

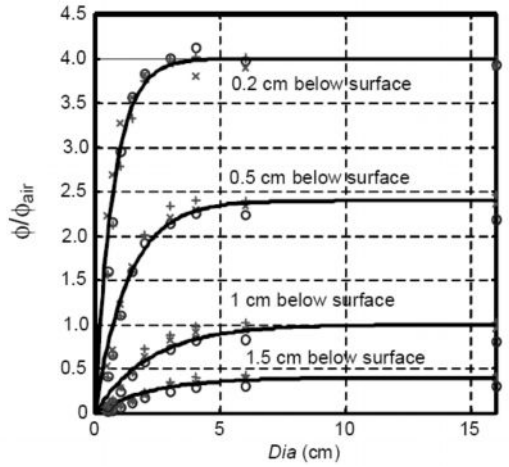

Fig.IV.2.4.3. *Comparison of measured (symbols) and Monte Carlo calculated (lines) Φ/Φ_{air} in a semi-infinite trubid medium (1% Intralipid, μ_a = 0.1 cm^{-1}) as a function circular field diameter, Dia = 2R. Symbols are for different wavelengths: o: 532 nm, +: 630 nm, and x: 730 nm. The MC simulation is made for μ_a = 0.1 cm^{-1}, μ_s = 13 cm^{-1}, g = 0.9, and n = 1.4.* [*Zhu &Dimofte et al 2003*]

The measured ratio of Φ/Φ_{air} agreed with Monte-Carlo simulation inside the tissue. The optical penetration depth δ starts to reduce significantly when the radius of circular field is less than 2 cm. The variation of Φ/Φ_{air} as a function of beam radius and depth was also demonstrated. One potential cause for the difference between the measurement and the Monte-Carlo simulation is the difference of index of refraction between water (n = *1.33*) and the tissue (n = *1.4*). The other possible cause of the difference between the measurement and the MC simulation is an overcorrection of the isotropic detector response inside tissue.

In-vivo light dosimetry agrees with Monte-Carlo simulation for small field dosimetry provided the isotropic detector is corrected for the blind spot. The light fluence rates for small circular fields are substantially lower than that of the broad beam of the same incident irradiance.

Chapter V The photodynamic therapy (PDT): application to the various cancer therapy

V.1. Prostate cancer treatment

V.1.1. In-vivo light dosimetry of interstitial PDT of human prostate [Zhu&Dimofte 2006]

Measurements were made in-vivo at the treatment wavelength (732nm) in 15 patients in three to four quadrants using isotropic detectors placed inside catheters inserted into the prostate. Cylindrical diffusing fibers (CDF) with various lengths are introduced into the catheters to cover the entire prostate gland. The length of the CDF at a particular position within the prostate was selected to cover the full length of the

prostate (see Fig. V.1.1.1a). The final plan required that the prostate be divided into four quadrants. Four isotropic detectors were used, each placed in the center of one quadrant. A fifth isotropic detector is placed in a urethral catheter to monitor the light fluence in the urethra (Fig. V.1.1.1b). To evaluate the distribution of light fluence rate, a point source was introduced in the prostate before and after PDT for selected patients. The distance dependence of light fluence rate was measured using a motorized isotropic detector [*Zhu 2005c*].

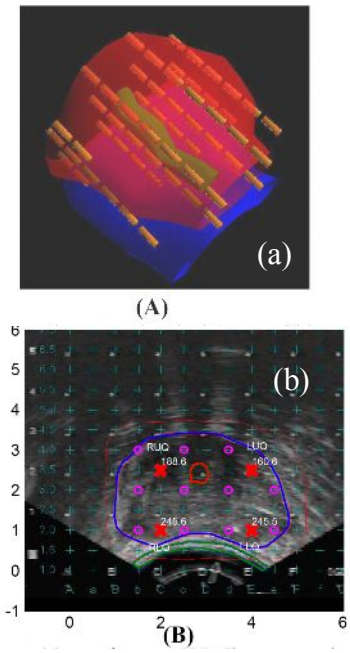

Figure V.1.1.1. (a) Schematic of placement of light source and detectors for prostate PDT. Cylindrical diffusing fibers (CDF) were inserted into the catheters to illuminate the entire prostate gland. Four isotropic detectors (not shown) are placed in one of the catheters to detect the light fluence rate.

(b) Schematics of the relative positions between a CDF and four isotropic detectors overlaid on the US image on the 0.5-cm Template for patient #13. The detector positions are labeled as RUQ, LUQ, RLQ, and LLQ for right upper quadrant, left upper quadrant, right lower quadrant, left lower quadrant, respectively. [*Zhu&Dimofte 2006*]

The optical properties measured in 13 patients have been published in [*Zhu&Dimofte 2005a*]. The variation within a prostate at different locations was as large as the variation among prostates. We attribute these variations to heterogeneity of optical properties. Large variations of depth dependence of light fluence rate per source power *(Φ/S)* were observed for point source measurements. Using the measured mean optical properties and the kernel-based fluence rate calculation, one can determine the 3D light fluence rate distribution for a specific source loading. Due to heterogeneity of the optical properties significant variations of light fluence rate were observed both intra and inter prostates.

The peak light fluence rate at the prescription point varied by 24 times (from 26 to 634mW/cm^2) for the same source loading at 732 nm, thus a real-time dosimetry system is necessary to quantify the light fluence rate *in vivo*.

The measurements were compared with calculations and found that light fluence rate calculation based on the mean homogeneous optical properties can predict the light fluence rate to a mean error of 85%. When calculation is performed based on heterogeneous optical properties, this agreement improved to 20%

To improve the agreement between calculation and measurement, it is necessary to take into account the distribution of optical properties within each patient.

V.1.2. Improvement of light dosimetry for prostate photodynamic therapy

Improvement of the light dosimetry can be obtained by optimization of the fluence rate calculation [*Li&Dimofte 2008]* and of the optical properties measurements [*Zhu&Dimofte 2005a*].

Two stages of the optimization of the optical properties measurements were done (1) one in which a point source light and (2) a second when a *linear source emitting 732 nm light* is used.

(1) Optical properties of human prostate at 732nm measured in vivo during Motexafin Lutetium (MLu) mediated PDT. [*Zhu&Dimofte 2005a*]

In the first stage of the optimization of the optical properties measurements, the prostate was illuminated with a ***point source emitting 732 nm light***. The main objective of the study is to evaluate the optical properties of prostate tissue in the human prostate using 732 nm light. Comparisons were made before, during and after MLu mediated PDT. Differences within and among patients were also studied. Differences in optical properties were compared before and after PDT in which the entire prostate was treated. The calibration procedure of the isotropic detector and the phantom verification is described in [*Zhu&Dimofte 2005a*]. A total of 14 patients were treated, of which 13 patients have undergone measurement of optical properties. Cylindrical diffusing fibers (CDF) with active lengths of 1, 2, 3, 4 and 5 cm were used as light sources. In figure V.1.2.1 the variation of the measured light fluence rate distribution along the catheter (solid lines, there are too many measured points to express the measured data clearly as symbols) and the associated fit (symbols) is shown for: (a) different locations in the same prostate gland and (b) the same location in a prostate before and after light delivery.

A large variation was also observed among different patients. The linear relationship between MLu drug concentration and the μ_a at 732 nm is consistent with

that observed in canine prostate at 732 nm, but a larger intersect (μ_a = 0.23 cm^{-1}) is found in humans than in dogs (μ_a = 0.08 cm^{-1}) [*Zhu&Dimofte 2003*].

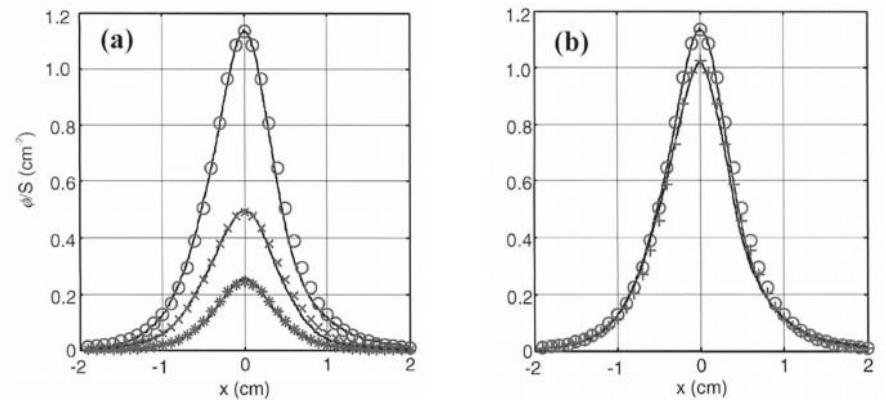

Figure V.1.2.1. *Measured light fluence rate per unit source strength (Φ/S) at distances along the catheter,* ***x*** *, from the point source measured in vivo in human prostate gland for atient13.*
(a) Light fluence rates in the right lower quadrant (O), right upper quadrant (x) and left upper quadrant (*) of the same prostate before PDT.
(b) Light fluence rates before (o) and after (+) light treatment in the right lower quadrant of the prostate gland.

(2) In the second stage of the optimization of the optical properties measurements, the prostate was illuminated with a *linear source emitting 732 nm light*. The results of this study were described in Chapter IV. 2.3.

V.2. Treatment of malignant pleural effusion (lung) cancer

In-vivo Light dosimetry for pleural PDT *[Dimofte 2009]*

The study [*Dimofte 2009*] described below examines the relationship between the PDT treatment time and thoracic treatment volume and surface area for patients undergoing pleural PDT. The light fluence (rate) delivered to patients undergoing pleural PDT as a function of treatment time, treatment volume and surface area, and its accuracy are discussed. All patients underwent thoracotomy. After resection, each patient received PDT to treat the thoracic cavity. 24 hours before the surgery each patient was injected with Photofrin (porfimer sodium) at a concentration of 2 mg/kg body weight. 630nm illumination was provided by a dye laser pumped by a KTP-YAG laser (*model 630 XP, Laserscope, Inc, San Jose, CA*) and was delivered via a diffusing

optical probe consisting of an optical fiber mounted in a modified endotracheal tube that terminated in a balloon filled with 0.1% intralipid. Patients were treated with laser light with a light fluence of 60J/cm^2 at 630nm. Fluence rate (mW/cm^2) and cumulative fluence (J/cm^2) was monitored at 7 different sites during the entire light treatment delivery.

The optical properties of various tissues in the thoracic cavity were measured using an optical probe. Figure V.2.2.1 shows how the red light is delivered to the patient and figure V.2.2.2. shows the light detectors sewn into left chest after parietal pleurectomy and pneumonectomy.

Fig. V.2.2.1. Delivery of the red light.

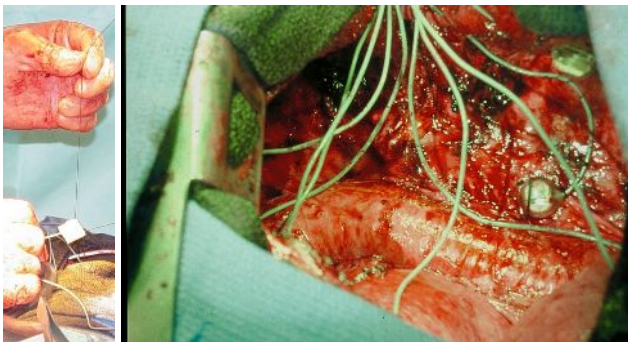

Fig. V.2.2.2. Light detectors sewn into the left chest after parietal pleurectomy and pneumonectomy

The entire procedure of the isotropic detector calibration is described in [*Dimofte 2009, 2010*].

Long term accuracy of in-vivo light dosimetry was determined by examining individual calibration accuracies of the integrating sphere used for detector calibration, and the overall calibration factor uncertainties over a long period of time.

To verify the accuracy of the expression used for the calculation of diffuse reflectance, a series of measurements were performed in water and liquid phantom interface. A comparison between the theory and the measurements is shown in Figure V.2.2.10, where Φ is the light fluence measured at the tissue surface and Φ_{air} is the incident light fluence. Good agreement between theory and experiment can be observed.

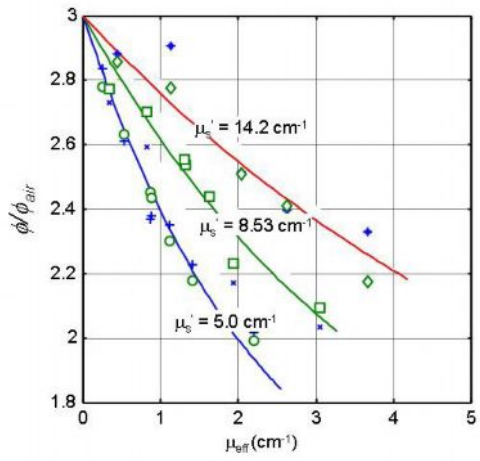

Figure V.2.2.10. Comparison between the theory and the measurement for diffuse reflectance by comparing the ratio of light fluence measured at the tissue surface $\boldsymbol{\Phi}$ *and the incident light fluence* Φ_{air}. $\Phi/\Phi_{air} = 1 + 2\rho$.

Using the measured diffuse reflectance, one can calculate the linear coefficient (*k)* between the treatment time and the treatment area. The *k* values generally decrease with increasing effective attenuation coefficient, however there is a wide spread because of the distribution of absorption and scattering coefficients.

A linear correlation between the total treatment time and the treatment area: *t (sec) = 4.80 A* (cm^2) was established. A similar correlation exists between the treatment time and the treatment volume: *t (sec) = 2.33 V* (cm^3). The results can be explained using an integrating sphere theory and the measured tissue optical properties assuming that the saline liquid has a mean absorption coefficient of 0.05 cm^{-1}. The results can be used as a clinical guideline for future pleural PDT treatment.

V.3. Treatment of head and neck cancer

The main purpose of this study was to determine the optical properties (scattering and absorption coefficients) in phantom and *in vivo* by interstitial measurements using a light detection device made for this purpose. The patients studied here were enrolled in a phase I dose escalation study of photodynamic therapy for the treatment of pre-malignant tumors and superficial microinvasive disease of the head and neck.

Validation measurements performed in optical phantom

The tissue simulating phantoms were made of Intralipid and ink of various concentrations: 0.23, 0.53, 1.14 and 1.91% intralipid and 0.002, 0.012, 0.023 and 0.034% ink. Optical properties were determined by measuring the ratio of light fluence rate to source power along a linear channel at a fixed distance (4 mm) from an isotropic point source. The light detection system consists of two parallel light transmitting catheters placed 4 mm apart. Diffuse light, from a 2mm cylindrical diffusing tip, is

collected by an isotropic detector with a 0.5 mm scattering bulb whose position is determined by a computer controlled step motor, with a positioning accuracy of better than 0.1 mm. The system automatically records and plots the light fluence rate per unit source power as a function of position. The result is fitted with a diffusion equation to extrapolate μ_a and μ_s'. Measurements where made in liquid tissue simulating phantoms, with known reduced scattering coefficient (μ_s') and absorption coefficient (μ_a). The diffusion theory based on light source on semi-infinite medium was used to interpret the measured data.; the method was described in chapter IV.

The experimental setups allow broad beam measurements and semi-infinite model measurements. A Matlab-based program was developed to analyze the measured scans and to extract the optical properties for the determination of the optical properties. The result is fitted with a diffusion equation to extract μ_a and μ_s'. Figures V.3.1 show the optical properties of one of the investigated phantom.

The optical properties were determined using broad-beam and parallel-catheter methods. A comparison between optical properties (μ_a, μ_s' *and* μ_{eff}) determined by broad-beam and parallel-catheter methods for different measurements done for optical phantoms with various Liposyn and ink concentrations is presented.

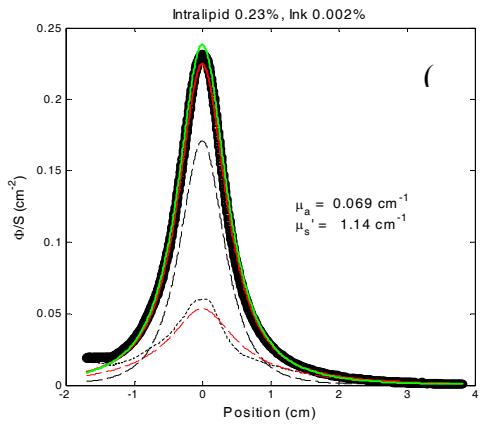

Figure V.3.1. Optical properties of the investigated phantom.

Clinical measurements

Patients in this study were treated with PDT for head and neck mucosal dysplasia. They were enrolled in a phase I study of escalating light doses and oral ALA with 60mg/kg. Red light at 630nm was administered to the tumor from a laser. The photosensitizer used is 5-aminolevulinic acid (5-ALA) [*Wilson 1992*], an intrinsic photosensitizer with no photosensitizing properties that is converted in situ to a photosensitizer called protoporphyrin IX. The light dose was escalated from 50 to 200J/cm^2. The light detection device (fig V3.2) consists of two parallel, 2mm (OD) light

transmitting catheters placed 5mm apart. In one of the catheters a 2 mm long linear diffusing light source is placed along the length of the catheter. In the second parallel catheter, a calibrated isotropic detector is placed along the length of the catheter.

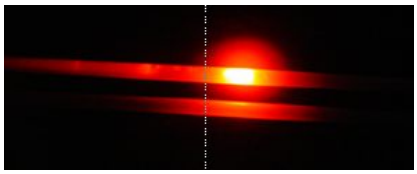

Figure V,3,2. Parallel catheter device used to measure tissue optical properties in H&N patients.

In figure V.3.3. the actual light delivery and optical property measurement picture during treatment for one of the head and neck patients is shown**.** The detectors were calibrated to measure absolute fluence rate in air and corrected for the effects of decreased refractive index mismatch in the liquid and solid phantoms. The treatment time was calculated based on the initial measured fluence rate.

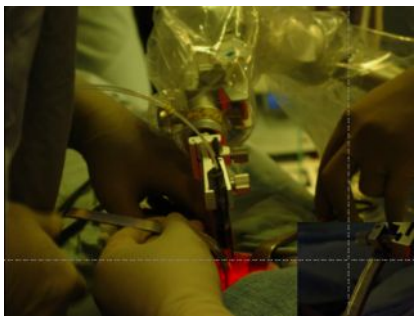

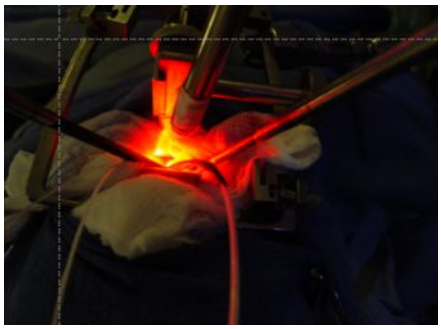

*Figure V.3.3 Actual light delivery and optical property measurement picture during treatment for one of the H &N patients***.**

The diffusely reflected white light was collected by a spectrograph and analyzed using a hybrid diffusion-P_3 model [*Hull 2001*] to determine the absorption and scattering spectra of the tissue. Results from the two methods were compared. The optical properties of the tumor and normal tissue were determined before and after PDT treatment using the parallel catheter method. Large heterogeneities were observed. Large variations of μ_{eff} were measured.

Conclusions

The results of the research conducted and presented in this work can be divided into two categories: (I) Studies relating to determination of the detector calibration factor used in PDT and of the optical properties of different tissues using various methods and (II) Application of the photodynamic therapy (PDT) in treating prostate, lung, head and neck cancer.

(I)

- The response of an isotropic detector as function of the indices of refraction of the surrounding medium was examined theoretically and experimental. Theoretical analysis and the experiments have demonstrated that the effect of intermediate medium is negligible.
- A method and a device to quickly determine the optical properties in tissue simulating liquid phantom are described. *In vivo* data measured in human prostate using this method is presented.
- The optical properties of prostate simulating phantoms were determined using linear sources instead of point source. Measurements were made on homogeneous and heterogeneous tissue-simulating phantoms with varying optical properties. The phantom optical properties were characterized using two independent methods.
- The spatial and time dependence of the measured light fluence rate *in situ* in patients enrolled in the ongoing Phase II trial of MLu mediated chest wall PDT for recurrent breast cancer were determined.
- The conversion factor was determined for five patients receiving MLu-mediated PDT. Significant increases (up to 2 times) in measured light fluence rate versus calculated incident fluence rate were observed, and consequently all PDT chest wall treatment protocols incorporate careful *in-vivo* light dosimetry.
- Treatment based on output of light alone seriously underestimates available light at tissue surface, which varies significantly depending on treatment patient optical properties and, to a lesser extent, patient contour, and may affect treatment outcome.
- In order to use PDT to treat surface small lesions the change of the light fluence rate with field size is investigated.

II

Prostate cancer treatment

- *In-vivo* light dosimetry of interstitial PDT of human prostate is presented.

Measurements of the optical properties were made *in-vivo* at the treatment wavelength (732nm) in 15 patients in three to four quadrants using isotropic detectors placed inside catheters inserted into the prostate. The measurements were compared with calculations. When calculation is performed based on heterogeneous optical properties, this agreement improved to 20%. To improve the agreement between calculation and measurement, it is necessary to take into account the distribution of optical properties within each patient.

- Improvement of light dosimetry for prostate PDT, like *optimization of the fluence rate calculation and of the optical properties measurements is described.* Comparisons were made before, during and after MLu mediated PDT in 14 patients. Substantial inter- and intra-patient heterogeneity was observed.

Pleural effusion (lung) cancer treatment

- Isotropic detectors were used for *in-vivo* light dosimetry; the detectors were sewn to the wall of the pleural cavity for monitoring the light dose at 7 sites.
- Using measured optical properties performed *in-vivo*, theoretical calculations were used to determine the relationship between the treatment time and the treatment area and compared to the measured results.
- Long term accuracy of in-vivo light dosimetry was determined by examining individual calibration accuracies of the integrating sphere used for detector calibration, and the overall calibration factor uncertainties over a long period of time.
- The relationship between the PDT treatment time and thoracic treatment volume and surface area for patients undergoing pleural PDT is established. The results can be used as a clinical guideline for future pleural PDT treatment.

Treatment of head and neck cancer

- The purpose of this study was to determine the optical properties *in vivo* by interstitial measurements, using a light detection device made for this purpose.
- Optical properties were measured in liquid tissue simulating phantoms, with known reduced scattering and absorption coefficients.
- The optical properties were determined using a broad-beam, a parallel-catheter and the absorption method and a comparison between optical properties were made.
- The diffusion theory based on light source on semi-infinite medium was used to interpret the measured data.

❖ Optical properties were measured *in-vivo* before and after PDT for both tumor and normal tissue for patients treated with head and neck mucosal dysplasia. Large heterogeneities were observed. Large variations of μ_{eff} were measured.

References

Cope	1988	Cope M. and Delpy D.T. Med. Biol. Eng. Comput. 26 (1988)289
Dimofte	2002	**Dimofte A**, Zhu TC, Hahn SM, and Lustig RA, *"In Vivo Light Dosimetry for Motexafin Lutetium-mediated PDT of Recurrent Breast Cancer,"* Lasers in Surgery and Medicine 31 (2002) 305-312 .
Dimofte et al.	2005	**A. Dimofte**, J. C. Finlay and T. C. Zhu, *"A method for determination of the absorption and scattering properties interstitially in turbid media,"* Physics in medicine and biology 50(10) (2005) 2291-2311
Dimofte et al	2008	**Dimofte A,** Finlay JC, Li J, and Zhu TC, *"Determination of optical properties in a heterogeneous turbid media using a cylindrical diffusing fiber,"* Proceedings of SPIE (San Jose, CA), **Vol. 6845**, 2008
Dimofte	2009	**A. Dimofte**, T. C. Zhu, J. C. Finlay, M. Cullighan, C. E. Edmonds, J. S. Friedberg, K. Cengel, and S. M. Hahn, *In-vivo Light dosimetry for pleural PDT* Proc. SPIE 7164 (2009) 132-144
Dimofte	2010	**Dimofte A,** T. C. Zhu, J. C. Finlay, M. Cullighan, C. E. Edmonds, J. S. Friedberg, K. Cengel, and S. M. Hahn, *In-vivo Light dosimetry for HPPH-mediated pleural PDT* Proc. SPIE 7551 (2010) 6pg
Farrell	1992	Farrell T J and Patterson M S , Med. Phys. 19 (1992) 879–88
Finlay& Dimofte	2004	Finlay, J. C., T. C. Zhu, **A. Dimofte**, D. Stripp, S. B. Malkowicz, R.Whittington, J. Miles, E. Glatstein and S. M. Hahn *,In vivo determination of the absorption and scattering spectra of the human prostate during photodynamic therapy.* Proc. SPIE 5315 (2004) 132-142
Finlay	2006	J. C. Finlay, T. C. Zhu, **A. Dimofte**, D. Stripp, S. B. Malkowicz, T. M. Busch and S. M. Hahn, *"Interstitial fluorescence spectroscopy in the human prostate during motexafin lutetium-mediated photodynamic therapy,"* Photochemistry and Photobiology 82 (2006) 1270-1278
Finlay& Dimofte	2006	J. C. Finlay, T. C Zhu, **A. Dimofte**, J. S. Friedberg, and S. M. Hahn, *Diffuse reflectance spectra measured in vivo in human tissues during Photofrin-mediated pleural photodynamic therapy* Proc. of SPIE vol 6139 (2006) 613900
Groenhuis	1983 a	Groenhuis RAJ, Ferwerda HA, Bosch JJT. App Opt 22 (1983)2456-2462.

Groenhuis	1983 b	Groenhuis RAJ, Bosch JJT, Ferwerda HA. *"Scattering and absorption of turbid materials determined from reflection measurements. 2: Measuring method and calibration".* App Opt. 22 (1983) 2463-2467.
Hillegersberg	1994	van Hillegersberg R, Kort W J and Wilson J H P Drugs 48 (1994) 510–27
Hull	2001	Hsi, R. A., A. Kapatkin, J. Strandberg, T. Zhu, T. Vulcan, M. Solonenko, C. Rodriguez, J. Chang, M. Saunders, N. Mason and S. Hahn *Photodynamic therapy in the canine prostate using motexafin lutetium*. Clin. Cancer Res. 7 (2001) 651-460.
Jacques	1987	SL Jacques and SA Prahl, Lasers Surg. Med. 6(1987) 494-503
Jacques	1998	Jacques S L, Photochem. Photobiol 67 (1998) 23-32
Li& Dimofte	2008	Jun Li, T. C. Zhu, X. Zhou, **Dimofte A**, and J. C. Finlay "Integrated light dosimetry system for prostate photodynamic therapy", Optical Methods for Tumor Treatment and Detection: Mechanisms and Techniques in Photodynamic Therapy XVII, edited by David Kessel, Proc. of SPIE Vol. 6845, 68450Q, (2008) 1605-7422/08/$18 • doi: 10.1117/12.763806
Marijnissen	1993	Marijnissen J P A 1993, PhD Thesis Universiteit Amsterdam
Patterson	1989 a	Patterson M S, Schwartz E. and Wilson B C, Proc. SPIE 1065 (1989) 115-122
Marijnissen	1996	Marijnissen JPA and Star WM, Phys Med Biol 41(1996) 1191
Schmitt	1990	Schmitt J. M. , Zhou G.X. , Walker E.C. and Wall R. T. , Multilayer model of photon diffussion in skin, J. Opt. Soc. Am. A 7 (1990) 2141-2153
Shimada	2001	Shimada M, Yamada Y, Itoh M, and Yatagai T, Phys Med Biol 46 (2001) 2397-2406
Steinke	1986	Steinke J. M. and Shephert A.P IEEE Trans. Biomed. Eng., 34 (1986) 826-833
Vulcan	2000	Vulcan TG, Zhu TC, Rodriguez CE, His RA, Fraker DL, Baas P, Murrer LH P, Star WM, Glatstein E, Yodh AG, and Hahn SM. Lasers Surg Med 2000; 26:292-30
Zhu& **Dimofte** et al	2003	Zhu T C, **Andreea Dimofte**, Stephen M Hahn, and Robert A Lustig *Light dosimetry at tissue surfaces for small circular fields,* Optical Methods for Tumor Treatment and Detection: Mechanisms and Techniques in Photodynamic Therapy XII, David Kessel, Ed, Proceedings of SPIE Vol. 4952 (2003) 56-67
Zhu& **Dimofte**	2003	Zhu T C, Hahn S M, Kapatkin A S, **Dimofte A**, Rodriguez C E, Vulcan T G, Glatstein Eand Hsi R A 2003 *In vivo optical properties of normal canine prostate at 732 nm using motexafin lutetium mediated photodynamic therapy* Photochem. Photobiol. 77 (2003) 81–88
Zhu& **Dimofte**	2005 a	Zhu T C**, Dimofte A**, Finlay F C, Stripp D, Bush T, Miles J, Whittington R, Malkowicz S B, Tochner Z, Glatstein E and Hahn S M, *Optical properties of human prostate at 732 nm measured in vivo during Motexafin Lutetium-mediated photodynamic therapy*. Photochem. Photobiol. 81(2005) 96–105

Zhu& **Dimofte**	2005 b	Zhu T C, **Dimofte A,** Finlay J C, Glatstein E and Hahn S M ,"*Detector calibration factor for interstitial in vivo light dosimetry using isotropic detectors with scattering tip"* Proc. SPIE 5689 (2005)174–85
Zhu	2005 c	Zhu T C, J. C. Finlay and S. M. Hahn, J. Photochem.PhotobioBiology B 79 (2005) 231-241
Zhu	2006	T. C. Zhu and J. C. Finlay, Photodiagnosis and photodynamic therapy 4 (2006) 234-246
Zhu& **Dimofte**	2006	Zhu T C, J. Lin, J C.Finlay, **Dimofte A,** D. Stripp, Malkowicz B and Hahn S M *,"In- vivo light dosimetry of interstitial PDT of human prostate"* Proc. SPIE 6139 (2006)61390L
Wilson	1986	B.C. Wilson and M S Patterson, Phys. Med Biol.31 (1986) 327-360